DOI: 10.17516/1997-1397-2022-15-1-80-87
УДК 538.9

Anisotropy of the Electromechanical Characteristics of SH-Waves and Lamb Waves in Yttrium Aluminum Borate Single Crystals

Pavel P. Turchin*
Siberian Federal University
Krasnoyarsk, Russian Federation
Kirensky Institute of Physics
Federal Research Center KSC SB RAS
Krasnoyarsk, Russian Federation
Sergey I. Burkov†
Vladimir I. Turchin‡
Oleg N. Pletnev
Marina Yu. Chulkova
Anastasia G. Nechepuryshina
Siberian Federal University
Krasnoyarsk, Russian Federation

Received 10.04.2021, received in revised form 10.06.2021, accepted 20.08.2021

Abstract. The anisotropy of the electromechanical properties of SH-waves and Lamb waves in yttrium aluminum borates, which are nonmagnetic representatives of the $RMe_3(BO_3)_4$ single crystals family (where R=Y, La-Lu; M=Fe, Al, Cr, Ga, Sc) with unique properties of magnetoelectrics and multiferroics, has been studied. In the process of the numerical simulation of the acoustic waves characteristics, the values of linear electromechanical constants of $YAl_3(BO_3)_4$ single crystals, previously measured by ultrasonic pulse echo and quasi-static methods, have been used.

Keywords: surface acoustic, SH and Lamb waves, piezoelectrics, multiferroics, yttrium aluminum borates.

Citation: P.P. Turchin, S.I. Burkov, V.I. Turchin, O.N. Pletnev, M.Yu. Chulkova, A.G. Nechepuryshina, Anisotropy of the Electromechanical Characteristics of SH-Waves and Lamb Waves in Yttrium Aluminum Borate Single Crystals, J. Sib. Fed. Univ. Math. Phys., 2022, 15(1), 80–87.
DOI: 10.17516/1997-1397-2022-15-1-80-87.

Introduction

Single crystals of the $RMe_3(BO_3)_4$ trigonal rare-earth oxyborates family (where R=Y, La-Lu; M=Fe, Al, Cr, Ga, Sc), depending on the composition and thermodynamic conditions, have piezoelectric, magnetoelectric and multiferroic properties [1–3]. Since giant magnetoelectric [4] and magnetodielectric [5] effects were discovered in ($RFe_3(BO_3)_4$) ferroborates, aluminum borates $RAl_3(BO_3)_4$ are promising for applications in laser technology [6–9]. Recently, there has been a growing interest in the study of the macroscopic physical properties of these crystals, primarily

*pturchin@sfu-kras.ru
† https://orcid.org/0000-0001-5198-2145
‡ https://orcid.org/0000-0001-5584-4794

for the study of microscopic magneto-elastic-electric interactions in them, as well as for expanding their applications in functional electronics [4, 5, 10–15].

Yttrium aluminum borate $YAl_3(BO_3)_4$ (point symmetry 32) in the series of oxyborates is a nonmagnetic single crystal and characterises the anisotropy of the elastic-electric interaction in them. Previously, we obtained experimental values of the electromechanical constants of this single crystal by echo-pulse ultrasonic [16] and quasi-static [16, 17] methods. This also gave an opportunity to study the anisotropy of the main characteristics of bulk (BAW) and surface (SAW) acoustic waves in yttrium aluminum borates. The present article studies the dispersion of the electromechanical characteristics of SH-waves and Lamb waves and assesses the surface effect on the magnitude of the electromechanical interaction in yttrium aluminum borates. Numerical simulation is based on the experimental values of electromechanical constants [16, 17].

1. Theory and values of material constants of a single crystal

SH-waves and Lamb waves propagation in a piezoelectric crystal plate is considered in the operating orthogonal coordinate system, in which the X_3 axis is directed along the outer normal to the surface of the medium occupying the space $X_3 \leqslant h$ and $X_3 \geqslant 0$, and the X_1 axis coincides with the direction of wave propagation. For the waves of small amplitude, the wave equation, electrostatic equations, and equations of state of the piezoelectric medium have the following form [18]:

$$\begin{aligned} &\rho_0 \ddot{U}_i = \tau_{ik,k}, \;\; D_{m,m} = 0. \\ &\tau_{ik} = C_{ikpq} e_{pq} - e_{nik} E_n, \\ &D_n = e_{nik} e_{ik} + \varepsilon_{nm} E_m. \end{aligned} \tag{1}$$

Equation (1) contains the following notations: ρ_0 is the crystal density, U_i is elastic displacements vector, e_{ij} and τ_{ij} are tensors of infinitesimal mechanical deformations and stresses, E_i and D_i are vectors of electric field strength and induction, C_{ijkl}, e_{ijk} and ε_{ij} are tensors of elastic, piezoelectric and dielectric constants. Hereinafter, summation over a twice repeating index is meant.

Acoustic waves propagation in a piezoelectric plate of h thickness must correspond to the boundary conditions [19] of equality to zero of the normal stress tensor components at the crystal-vacuum interface. The continuity of the tangential to the interface components of the electric field strength vector is provided by the condition of continuity of the electric potential φ, as well as by the condition of continuity of normal components of the induction vector [20].

The detailed description of experimental studies of the values of elastic, piezoelectric, and dielectric constants is given in [16]. The elastic constants were found by solving the inverse problem of crystal acoustics [21] from the measured values of the BAW velocities in the basic and rotated crystallographic directions. To determine BAW velocities, an echo-pulse ultrasonic acoustic method, with an accuracy of 10^{-4} for absolute measurements, has been used. The measurements were performed at a frequency of 28 MHz. The absolute values of the piezoelectric constants have also been found from the measured values of the BAW velocities, but for piezoactive acoustic modes [16]. To clarify the values of the piezoelectric constants, quasi-static measurements of the d_{ijk} piezomodules, which are related with e_{ijk} by the equation [22] have been carried out

$$e_{ijk} = d_{ilm} C^E_{lmjk}. \tag{2}$$

In this method, a DMA 242 C device was used to create a precision variable dynamic loading. The signs of the piezoelectric constants were found by the direct measurement of the piezoelectric effect in the crystallophysical coordinate system, where $C_{14} < 0$. The high-frequency dielectric

permittivity is determined from the low-frequency one, taking into account the piezoelectric contribution.

Table 1. Values of electromechanical constants of $YAl_3(BO_3)_4$ single crystals at room temperature

Elastic constants $C_{\lambda\mu}$, 10^{10} N/m^2						
C_{11}	C_{12}	C_{13}	C_{14}	C_{33}	C_{44}	C_{66}
40.47±0.05	21.14±0.05	9.75±0.05	–2.35±0.1	27.09±0.05	7.49±0.01	9.67±0.05
Piezoelectric constants $e_{i?}, C/m^2, d_{i?}, 10^{-12}C/N$				Dielectric constants $\varepsilon_{ij}/\varepsilon_0$		
e_{11}	e_{14}	d_{11}	d_{14}	ε_{11}^{η}		ε_{33}^{η}
–1.06±0.07	–0.27±0.04	–6.0±0.3	–7.2±0.4	11.7±0.1		11.1±0.1

The experimental values of the linear electromechanical constants for $YAl_3(BO_3)_4$ single crystals are given in the Tab. 1.

2. Anisotropy of velocities and electromechanical coupling coefficients of SH-waves and Lamb waves

Lamb and SH-waves velocity values were found by solving equations (1) subject to boundary conditions [19, 20], taking into consideration the material constants' values given in the Table. The values of the electromechanical coupling constant K^2 was calculated according to the formula:

$$K^2 = 2\frac{(v - v_m)}{v}, \tag{3}$$

where v_m is the phase velocity on the metallized surface, and in the case of Lamb waves of both metallized surfaces.

Fig. 1 shows the dispersion dependences of the phase velocities and K^2 of the Lamb and SH-waves in Z and Y-cuts in the direction [100] and X-cuts in the direction [001] of the elastic wave propagation. The range of the considered values of h×f (thickness×frequency) is from 0 to 18000 m/s. The range of the phase velocities variation of Lamb and SH-waves is from the value of the phase velocity of the quasi-longitudinal BAW 10573 m/s to 3959 m/s SAW in Z and Y-cuts. But in X-cut, the range of Lamb and SH-waves phase velocity variations is from 8533 m/s (QL) to 4228 m/s (SAW). In this case, all elastic wave modes are piezoactive. The maximum K^2 value for the fundamental mode is achieved for the S_0 mode of the Lamb wave in Z and Y-cuts in h×f range from 250 m/s to 3000 m/s and $K^2 = 0.09$ for the Y-cut when h×f = 2250 m/s, but in Z-cut K^2=0.026 (Fig. 1d, e). It should be noted that in Y-cut for all elastic wave modes K^2 values are almost three times higher than the corresponding values in Z-cut. In X-cut, the maximum value for the S_0 mode is K^2= 0.003 when h×f = 4450 m/s. The situation with the antisymmetric mode A_0 is similar. The maximum $K^2 = 0.042$ (Fig. 1f) in X-cut is achieved for the SH_0 mode when h×f = 1650 m/s. It is necessary to note that the obtained K^2 values are significantly higher than those obtained in langasite single crystals [23].

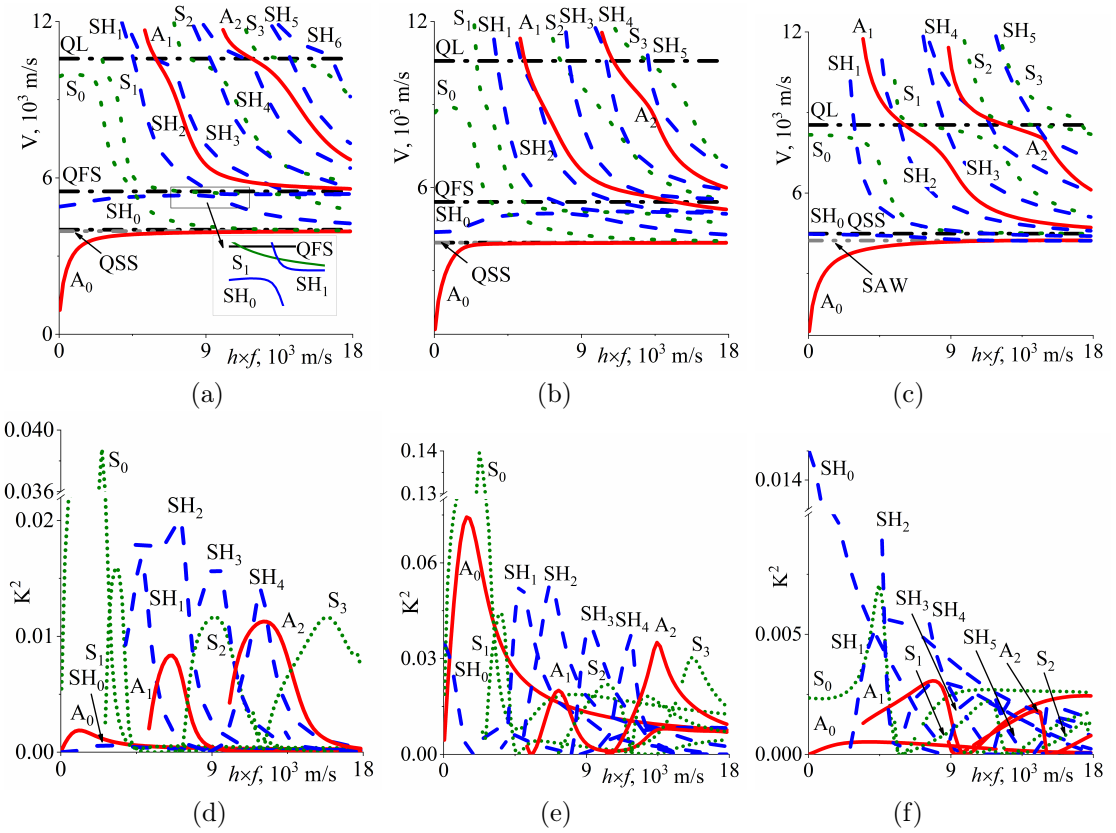

Fig. 1. Dispersion dependences of phase velocities and K^2 of Lamb and SH-waves: a, d) Z-cut; b, e) Y-cut; c, f) X-cut

One of the features of Lamb waves propagation in these cuts is the presence of interaction (hybridization) regions [24] between the Lamb wave modes, in which a significant change in the K^2 values of the interacting modes of the elastic wave takes place. For example, in the Z-cut between S_1 and SH_2 modes when h×f = 6050 m/s or S_2 and SH_3 when h×f = 9650 m/s. The peculiarity of the phase velocities in the interaction region of elastic wave modes is reflected in the tab in Fig. 1a. Hybridization is manifested more significantly in X-cut, where interaction occurs only between the S_0 and A_1 modes when h×f = 7050 m/s and 9750 m/s. Moreover, K^2 changes of the S_0 mode in the hybridization region occur from $K^2 = 0.03$ to $K^2 = 0.006$. However, it should be noted that in Y-cut there is an interaction only between the S_0 and SH_0 modes, where the K^2 change is insignificant.

Fig. 2 shows the anisotropy of phase velocities and K^2 in Z-cut of the $YAl_3(BO_3)_4$ crystal of Lamb and SH-waves at values h×f = 1050, 6050, and 10650 m/s. Along with the fundamental modes of the Lamb wave, Fig. 2a, d) demonstrates phase velocities and the K^2 of nondispersive acoustic BAW and SAW. The maximum values $K^2 = 0.104$ are achieved for the fast shear wave QFS at an angle of 30° with the direction [100]. The maximum value $K^2 = 0.07$ is also achieved for the SH_0 mode in the same direction. For quasi-longitudinal BAW, as well as for the S_0 mode, the maximum K^2 value in the direction of the elastic wave propagation [100] is K^2=0.03 and $K^2 = 0.024$, correspondingly. It should be noted that the minimum K^2 values in the $YAl_3(BO_3)_4$ plate are for SAW, which does not exceed the value $K^2 = 0.0013$.

With an increase in the h×f values, the K^2 value of the Lamb wave modes decreases

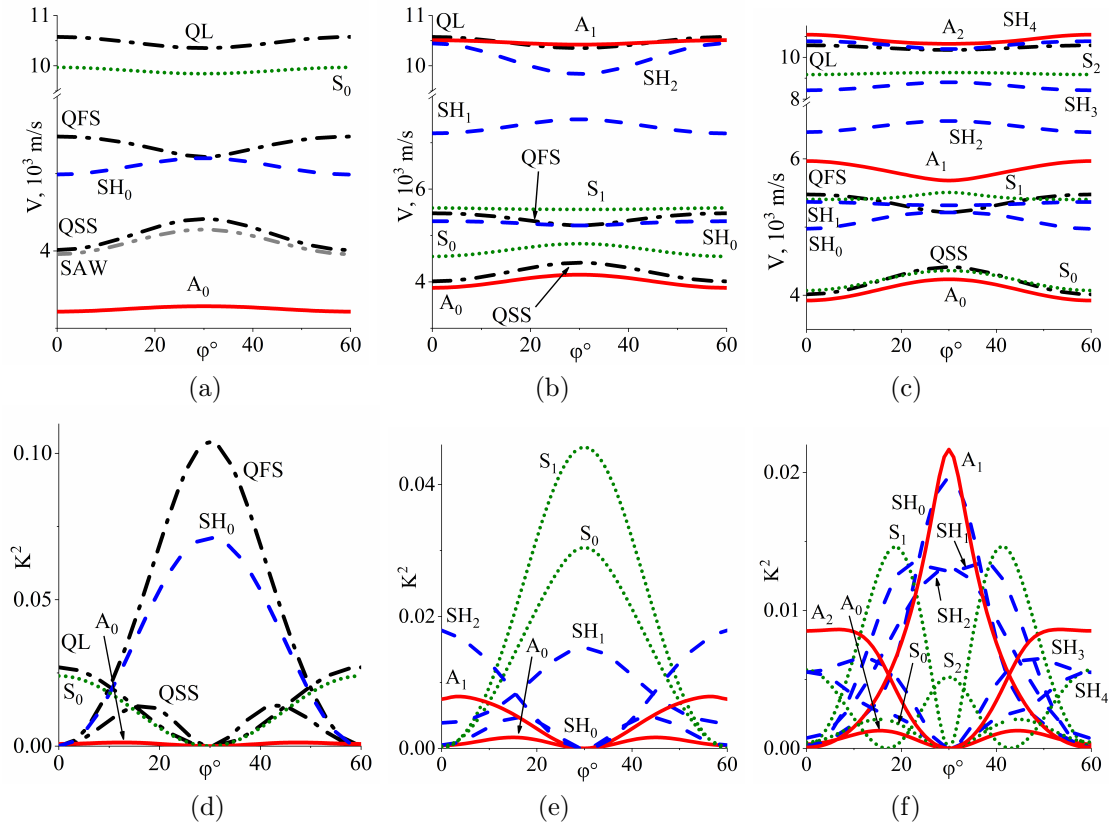

Fig. 2. Anisotropy of phase velocities and K2 of Lamb waves in Z-cut $(\varphi^\circ, 0^\circ, 0^\circ)$ of the YAB crystal plate at different values of thickness×frequency a, d) h×f= 1050 m/s; b, e) h×f= 6050 m/s; c, f) h×f = 10650 m/s

(Fig. 2e, f). Moreover, the maximum K^2 values are for SH-waves and antisymmetric A_1. For example, the K^2 values of the elastic wave modes A_1, SH_0 and SH_1 at an angle of 30° with the direction [100] are 0.008, 0.018, 0.02 (Fig. 2e) when h×f = 6050 m/s, correspondingly. However, when h×f = 10650 m/s K^2 = 0.014 for the SH_0 mode (Fig. 2f).

Fig. 3 shows the anisotropy of phase velocities and K^2 of Lamb and SH-waves in Y-cut of the $YAl_3(BO_3)_4$ crystal when h×f =1050, 6050, and 10650 m/s. In Y-cut, all BAWs are also piezoactive, but the maximum ECC value is achieved for a longitudinal wave QL in the direction [100] K^2=0.03. For non-dispersive SAW, the maximum ECC value K^2=0.011 is achieved in the direction of an elastic wave propagation at an angle of 28° with the axis [100]. For the fundamental modes of the Lamb wave, the maximum ECC values when h×f = 1050 m/s for the elastic wave modes S_0, A_0 and SH_0 are 0.074, 0.026, and 0.004, correspondingly (Fig. 3 d). It should be noted that the maximum K^2 values are achieved in Y-cut.

As h×f increases, the ECC values decrease for all elastic wave modes. However, in Y-cut, an interaction between the elastic wave modes also arises, and leads to a sharp change in the K^2 values of interacting modes in the hybridization region (Fig. 3 e, f). For example, between the elastic wave modes SH_0 and S_1 when h×f = 6050 m/s or SH_0 and A_1, SH_2 and S_1 when h×f = 10650 m/s (Fig. 3 e, f). It should also be noted that in the direction [001] of acoustic wave propagation, the maximum K^2 value when h×f =6050 m/s is achieved for the elastic wave mode SH_1 K^2=0.034, while the other modes have close to zero K^2 values.

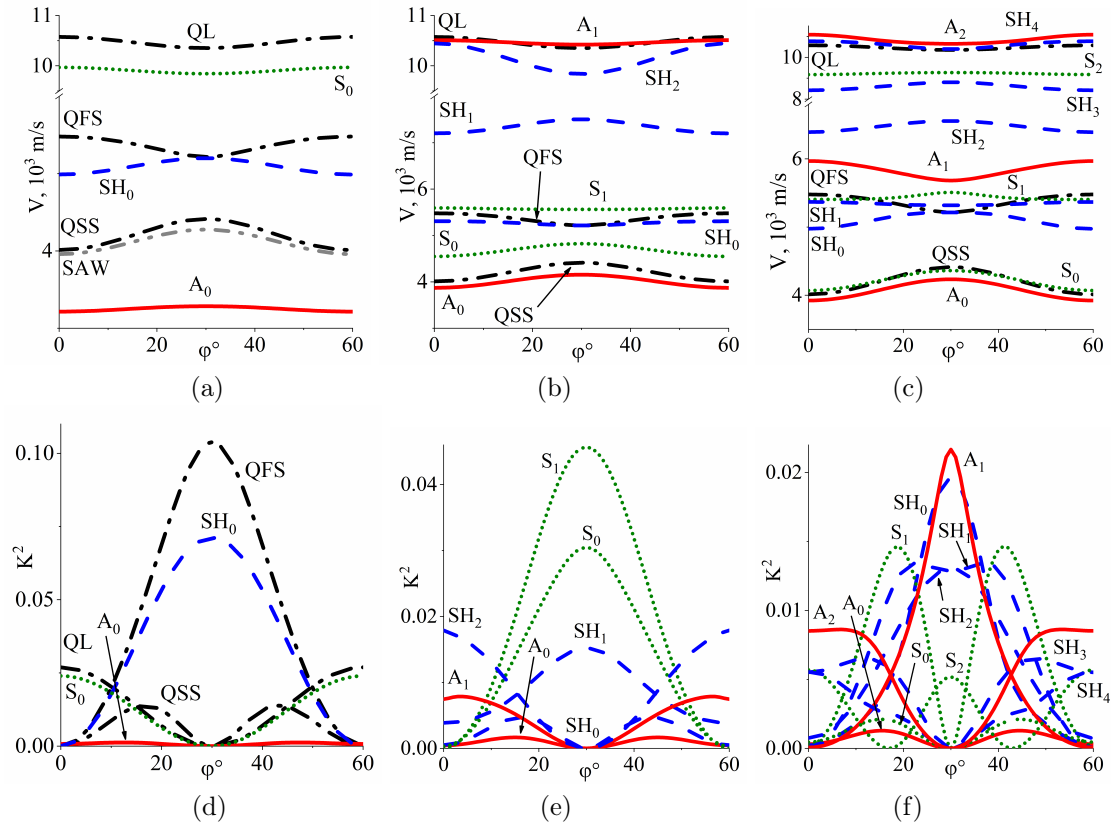

Fig. 3. Anisotropy of phase velocities and K^2 of Lamb waves in Y-cut $(0°, 90°, \psi°)$ of the YAB crystal plate at different values of thickness×frequency a, d) h×f = 1050 m/s; b, e) h×f = 6050 m/s; c, f) h×f = 10650 m/s

Conclusion

In this study, the values of elastic and piezoelectric material constants obtained by acoustic and quasi-static measurements are used to study the electromechanical characteristics of acoustic waves: bulk, surface, SH-waves, and Lamb waves in the plates of yttrium aluminum borate single crystals. The range of changes in phase velocities (from 800 m/s to 11800 m/s) and the maximum value of the electromechanical coupling coefficient ($K^2 = 0.14$ for the S_0 mode at Euler angles of $0°, 90°, 0°$) have been established. The propagation directions and h×f values for which hybridization of acoustic waves is observed have been found in the cuts under study. The phase velocities of Lamb and SH-waves, as well as K^2 waves significantly exceed the similar ones in langasite single crystals [23].

The study was carried out within the framework of the state assignment of the Ministry of Science and Higher Education of the Russian Federation (research project code FSRZ-2020-0011).

References

[1] D.Khomskii, Trend: Classifying multiferroics: Mechanisms and effects, *Physics*, **2**(2009), no. 20. DOI: 10.1103/Physics.2.20

[2] R.Ramesh, N.A.Spaldin, Multiferroics: progress and prospects in thin films, Nanoscience and Technology: A Collection of Reviews from Nature Journals, 2010, 20–28. DOI: 10.1142/9789814287005_0003

[3] N.A.Spaldin, M.Fiebig, The renaissance of magnetoelectric multiferroics, *Science*, **309**(2005), no. 5733, 391–392. DOI: 10.1126/science.1113357

[4] K.C.Liang et al, Giant magnetoelectric effect in $HoAl_3(BO_3)_4$, *Physical Review B*, **83**(2011), no. 18, 180417. DOI: 10.1103/PhysRevB.83.180417

[5] A.A.Mukhin et al,. The giant magnetodielectric effect in the multiferroic $SmFe_3(BO_3)_4$, *Letters to the Journal of Experimental and Theoretical Physics*, **93**(2011), no. 5, 305–311. DOI: 10.1134/S0021364011050079

[6] K.N.Girbachenya et al., High-frequency Er^{3+}, Yb^{3+}: $YAl_3(BO_3)_4$ microchip laser with longitudinal diode pumping, *Devices and methods of measurement*, **2**(2012), no. 5, 79–81.

[7] A.S.Aleksandrovsky et al., Upconversion luminescence of $YAl_3(BO_3)_4$:(Yb^{3+}, Tm^{3+}) crystals, *Journal of Alloys and Compounds*, **496**(2010), no. 1-2, 18–21. DOI: 10.1016/j.jallcom.2010.02.089

[8] G.Wang et al, Cr^3-doped borates-potential tunable laser crystals? *Radiation Effects and Defects in Solids*, **136**(1995), no. 1-4, 43–46. DOI: 10.1080/10420159508218789

[9] L.Zheng et al., >1 MW Peak Power at 266 nm in Nonlinear $YAl_3(BO_3)_4$ (YAB) Single Crystal, In Lasers and Electro-Optics (CLEO), 2015 Conference on. IEEE, 2015. DOI: 10.1364/CLEO_AT.2015.JTu5A.33

[10] N.V.Volkov et al., Magnetization, magnetoelectric polarization and specific heat of $HoGa_3(BO_3)_4$, *JETP Letters*, **99**(2014), no. 2, 67–75. DOI: 10.1134/S0021364014020106

[11] A.I.Popov, D.I.Plokhov, A.K.Zvezdin, Quantum theory of magnetoelectricity in rare-earth multiferroics: Nd, Sm, and Eu ferroborates, *Physical Review B.*, **87**(2013), no. 2, 024413. DOI: 10.1103/PhysRevB.87.024413

[12] A.K.Zvezdin et al., On magnetoelectric effects in gadolinium ferroborat $GdFe_3(BO_3)_4$, *JETP Letters*, **81**(2005), no. 6, 272–276. DOI: 10.1134/1.1931014

[13] T.N.Gaydamak et al., Elastic and piezoelectric moduli of Nd and Sm ferroborates, *Low Temperature Physics*, **41**(2015), no. 8, 614–618. DOI: 10.1063/1.4929719

[14] V.I.Zinenko et al., Vibrational spectra, elastic, piezoelectric and magnetoelectric properties of $HoFe_3(BO_3)_4$ and $HoA1_3(BO_3)_4$ crystals, *Journal of Experimental and Theoretical Physics*, **117**(2013), no. 6, 1032–1041. DOI: 10.1134/S1063776113140203

[15] G.A.Vziagina et al., Magnetoelastic effects in terbium ferroborate, *Low Temperature Physics*, **34**(2008), no. 11, 901–908. DOI: 10.1063/1.3009584

[16] P.P.Turchin et al., Electromechanical Properties and Anisotropy of Acoustic Waves Characteristics in Single Crystals $YAl_3(BO_3)_4$, *Journal of Siberian Federal University. Mathematics & Physics*, **12**(2019), no. 6, 756–771. DOI: 10.17516/1997-1397-2019-12-6-756-771

[17] P.P.Turchin et al., Application of DMA 242 C for Quasi-Static Measurements of Piezoelectric Properties of Solids, *Journal of Siberian Federal University. Mathematics & Physics*, **13**(2020), no. 1, 97–103. DOI: 10.17516/1997-1397-2020-13-1-97-103

[18] D.Royer, E.Dieulesaint, Elastic waves in solids II: generation, acousto-optic interaction, applications, Springer Science & Business Medial, 1999.

[19] I.A.Viktorov, Rayleigh andLamb Waves, Springer US, 1967.

[20] J.Rajagopalan, K.Balasubramaniam, C.V.Krishnamurthy, A phase reconstruction algorithm for Lamb wave based structural health monitoring of anisotropic multilayered composite plates, *The Journal of the Acoustical Society of America*, **119**(2006), no. 2, 872–878. DOI: 10.1121/1.2149775

[21] K.S.Aleksandrov, G.T.Prodaivoda, Anisotropy of the elastic properties of minerals and rocks, Novosibirsk, Publishing house of the SB RAS, 2000.

[22] J.F.Nye et al., Physical properties of crystals: their representation by tensors and matrices, Oxford university press, 1985.

[23] S.I.Burkov, O.P.Zolotova, B.P.Sorokin, P P.Turchin, Calculation of Thermostable Directions and the Effect of External Electric Field on the Propagation of Lamb and SH Waves in a Langasite_Crystal Plate, *Acoustical Physics*, **58**(2012), no. 6, 650–657. DOI: 10.1134/S1063771012050065

[24] I.E.Kuznetsova, B.D.Zaytsev, A.A.Teplykh, I.A.Borodina, Hybridization of acoustic waves in piezoelectric plates, *Acoustical Physics*, **53**(2007), no. 1, 64–69. DOI: 10.1134/S1063771007010071

Анизотропия и электромеханические характеристики SH-волн и волн Лэмба в монокристаллах иттриевого алюмобората

Павел П. Турчин
Сибирский федеральный университет
Красноярск, Российская Федерация
Сергей И. Бурков
Владимир И. Турчин
Олег Н. Плетнев
Марина Ю. Чулкова
Анастасия Г. Нечепурышина
Сибирский федеральный университет
Красноярск, Российская Федерация

Аннотация. Исследована анизотропия электромеханичеких характеристик SH-волн и волн Лэмба в иттриевых алюмоборатах, которые являются немагнитным представителем семейства монокристаллов $RMe_3(BO_3)_4$ (где R=Y, La-Lu; M=Fe, Al, Cr, Ga, Sc) с уникальными свойствами магнитоэлектриков и мультиферроиков. При численном моделировании характеристик акустических волн использованы значения линейных электромеханических постоянных монокристаллов $YAl_3(BO_3)_4$, измеренных ранее ультразвуковым эхо-импульсным и квазистатическим методами.

Ключевые слова: поверхностные акустические, SH- и Лэмба волны, пьезоэлектрики, мультиферроики, алюминоборат иттрия.